 doi:10.20944/preprints201906.0194.v1

Article

Ectopic Lipid Accumulation is Key Feature in Early Stages of Wooden Breast

Juniper A. Lake [1], Michael B. Papah [2] and Behnam Abasht [3,*]

[1] Center for Bioinformatics and Computational Biology, University of Delaware, Newark, DE, United States of America; dnovick@udel.edu
[2] Department of Animal and Food Sciences, University of Delaware, Newark, DE, United States of America; papah@udel.edu
[3] Department of Animal and Food Sciences, University of Delaware, Newark, DE, United States of America; abasht@udel.edu
* Correspondence: abasht @udel.edu; Tel.: +01-302-831-8876 (B.A.)

Abstract: Wooden breast is a muscle disorder affecting modern commercial broiler chickens that causes a palpably firm pectoralis major muscle and severe reduction in meat quality. Most studies have focused on advanced stages of wooden breast apparent at market age, resulting in limited insights into the etiology and early pathogenesis of the myopathy. Therefore, the objective of this study was to identify early molecular signals in the wooden breast transcriptional cascade by performing gene expression analysis on the pectoralis major muscle of two-week-old birds that may later exhibit the wooden breast phenotype by market age at 7 weeks. Biopsy samples of the left pectoralis major muscle were collected from a subset of 101 birds randomly selected from a total of 302 birds at 14 days of age, after which all birds were raised to 7 weeks of age for scoring of wooden breast. RNA sequencing was performed on 5 unaffected and 8 affected female chicken samples, selected based on wooden breast scores (0 to 4) assigned at necropsy where affected birds had scores of 2 or 3 (mildly or moderately affected) while unaffected birds had scores of 0 (no apparent gross lesions). Differential expression analysis identified 60 genes found to be significant at an FDR-adjusted p value of 0.05. Of these, 26 were previously demonstrated to exhibit altered expression or genetic polymorphisms related to glucose tolerance or diabetes mellitus in mammals. Additionally, 9 genes have functions directly related to lipid metabolism and 11 genes are associated with adiposity traits such as intramuscular fat and body mass index. This study suggests that wooden breast disease is first and foremost a metabolic disorder characterized primarily by ectopic lipid accumulation in the pectoralis major.

Keywords: wooden breast; broilers; myopathy; breast muscle

1. Introduction

Wooden breast is one of several muscle abnormalities of modern commercial broiler chickens that causes substantial economic losses in the poultry industry due to its impact on meat quality. Emerging evidence suggests wooden breast may also be detrimental to bird welfare as affected chickens exhibit increased locomotor difficulties, decreased wing mobility, and higher mortality rates [1–3]. While the etiology of the myopathy is still poorly understood, many believe it to be a side-effect of improved management practices and selective breeding for performance traits due to increased susceptibility among broilers with high feed efficiency [4,5], breast muscle yield [4,6,7], breast muscle thickness [6,8], and growth rate [9,10], including growth rate during the first 1-2 weeks post-hatch [2].

Macroscopic manifestations of the disorder include pale and hardened areas, subcutaneous and fascial edema, petechial hemorrhages, spongy areas with disintegrating myofiber bundles, and white fatty striations characteristic of white striping [2,11]. An early study of wooden breast characterized its microscopic presentation as polyphasic myodegeneration and necrosis with regeneration and

 doi:10.20944/preprints201906.0194.v1

interstitial connective tissue accumulation (fibrosis), primarily affecting the cranial end of the pectoralis major muscle [11]. However, it has since been demonstrated that venous inflammation (phlebitis) and perivascular lipid and inflammatory cell infiltration appear in the first week of age and precede other symptoms [2]. Differential gene expression analysis of the pectoralis major in 7-week-old broilers suggests that hypoxia, oxidative stress, fiber-type switching, and increased intracellular calcium may be important components of the myopathy [12]. In two- and three-week old birds, differentially expressed genes were mostly associated with increased inflammation, vascular disease, increased oxidative stress, extracellular matrix remodeling, dysregulation of carbohydrates and lipids, and impaired excitation-contraction coupling [13]. Metabolomic profiling is in agreement with these results and provides evidence of oxidative stress and dysregulated carbohydrate and lipid metabolism in affected birds at 7 weeks of age [14].

The objective of the present study was to better characterize the transcriptional anomalies that exist in the pectoralis major of two-week-old birds that later develop wooden breast by market age at 7 weeks. Only one other gene expression study has investigated early stages of wooden breast [13]. The current study serves as a continuation of that work, but makes two key changes. First, unlike the previous study that used only male birds, we included only female birds in the RNA-seq analysis. Second, birds in the affected group all possessed mild or moderate wooden breast phenotypes rather than severe symptoms, which allowed us to capture a clearer signal of the earliest transcriptomic perturbations.

2. Materials and Methods

2.1 Experimental Animals and Tissue Collection

The University of Delaware Institutional Animal Care and Use Committee approved the animal conditions and experimental procedures used in this scientific study under protocol number 48R-2015-0. For this experiment, 302 mixed male and female Cobb500 broilers were raised according to industry growing standards in two poultry houses from 1 day to 7 weeks of age with free access to feed and water. Biopsy samples of the craniolateral area of the left pectoralis major muscle were collected from 101 randomly selected birds at 14 days of age in the same manner described by a previous study [13]. After biopsy, all birds were grown out to 7 weeks of age, at which time they were euthanized by cervical dislocation. During necropsy, the pectoralis major muscles were evaluated for gross lesions and palpable firmness associated with wooden breast and each bird was assigned a wooden breast score using a 0-4 scale; 0-Normal indicates the bird had no macroscopic signs of the myopathy, 1-Minimal indicates 1% or less of the breast muscle was affected, 2-Mild indicates between 1% and 10% of the breast muscle was affected, 3-Moderate indicates between 10% and 50% of the breast muscle was affected, and a score of 4-Severe indicates that more than 50% was affected. This scoring system is slightly different from the one previously used in our laboratory and separates unaffected, mildly and moderately affected chickens with a higher resolution.

2.2 Sample Selection and RNA-Sequencing

Selection of samples for use in RNA-seq analysis was based on wooden breast scores assigned at necropsy. A total of 6 unaffected and 8 affected birds were identified; affected birds had scores of 2 or 3 (mildly or moderately affected) while unaffected birds had scores of 0 (no apparent gross lesions). Only samples taken from female birds were used because there was an insufficient number of male birds that were classified as unaffected. Total RNA was extracted from pectoralis major tissue samples using the mirVana miRNA Isolation Kit (Thermo Fisher Scientific) according to the manufacturer's protocol and stored at -80°C until cDNA library preparation. Each RNA sample was quantified using the NanoDrop 1000 Spectrophotometer (Thermo Fisher scientific) and quality was assessed with the Fragment Analyzer at the Delaware Biotechnology Institute (DBI). cDNA libraries were constructed using the ScriptSeq Complete Kit (Human/Mouse/Rat) (Illumina) with the optional step of adding a user-defined barcode to the library. The 14 barcoded cDNA libraries were normalized and 10 µl of each sample were pooled in two tubes (7 samples in each pool). Pooled

 doi:10.20944/preprints201906.0194.v1

libraries were subsequently submitted to the DBI for paired-end 2x76-nucleotide sequencing on two lanes of a flow cell using the HiSeq 2500 Sequencing System (Illumina).

Raw sequencing reads were demultiplexed and then checked for quality using FastQC v0.11.7 [15]. All samples passed the quality check and were submitted to Trimmomatic v0.38 [16] to trim leading and trailing bases with quality below 20, remove reads with an average quality below 15, and remove reads that were shorter than 30 bases in length. Trimmed reads were then mapped to both Gallus_gallus-5.0 (Ensembl release 94) and GRCg6a (Ensembl release 95) chicken reference genomes using HISAT2 v2.1.0 [17] with concordant mapping required for both reads in each pair. Cuffdiff v2.2.1 [18] was used with the fragment bias correction option to identify differentially expressed genes between affected and unaffected birds. Genes were considered statistically significant if the FDR-adjusted p-value was ≤ 0.05. The use of two reference genome builds, the latter of which was released during the course of this study, provided validation of our results and allowed us to capture differentially expressed genes that may have borderline statistical significance due to assembly errors or bias. One sample (animal ID 424183) in the unaffected group displayed an extreme outlier expression pattern; it was therefore removed and differential expression analysis with Cuffdiff was repeated without this sample (5 unaffected vs. 8 affected). In order to compile the results generated from each reference genome, Ensembl gene IDs from Gallus-gallus-5.0 were mapped to GRCg6a gene IDs using Ensembl's ID History Converter; differentially expressed genes with annotation differences between the two reference genome releases were scrutinized for consistency. Pairwise correlation analysis and visualization of differentially expressed genes was conducted with the "stats" and "corrplot" packages [19] in R only using expression data generated with the GRCg6a reference genome build.

3. Results

An average of 19,616,353 paired-end sequence reads were generated per sample, which was reduced to an average of 19,609,044 paired-end reads after trimming. The average mapping rate per sample was 74.5% with the Gallus_gallus-5.0 reference genome build and 75.1% with GRCg6a. The total number of sequenced reads, trimmed reads, and mapped reads per sample can be found in Table S1.

There were 52 differentially expressed genes identified using the Gallus_gallus-5.0 reference genome build and 29 differentially expressed genes using the GRCg6a genome build. After accounting for changes in annotation of Ensembl Gene IDs between genome releases, a total of 60 genes were found to be differentially expressed between affected and unaffected groups across both analyses, with 18 differentially expressed genes overlapping between both Gallus_gallus-5.0 and GRCg6a. Three Ensembl Gene IDs from the earlier build were deprecated in GRCg6a and were excluded from further analysis. Of the 60 differentially expressed genes used for downstream analysis, 52 were upregulated in affected birds and 8 were downregulated in affected birds (Table 1).

Table 1. Differentially expressed genes between wooden breast affected pectoralis major muscle samples and unaffected samples at 2 weeks of age. Log2FC is calculated by log2(FPKMaffected/FPKMunaffected). Unknown gene names are indicated with a dash (-). Non-significant p-values (i.e. FDR-adjusted p-values > 0.05) are indicated as n.s.

Gene ID	Gene Symbol	Gene Name	Log2FC Galgal5	Log2FC GRCg6a
		Genes upregulated in affected group		
ENSGALG00000046652	-	-	1.55	n.s.
ENSGALG00000052084	-	-	n.s.	2.06
ENSGALG00000006491	ANKRD1	Ankyrin repeat domain 1	1.28	0.99
ENSGALG00000049422*	ATF3	Activating transcription factor 3	1.04	n.s.
ENSGALG00000009846	BBS5	Bardet-Biedl syndrome 5	0.76	n.s.
ENSGALG00000017040	C4A	Complement C4A (Rodgers blood group)	1.24	0.96
ENSGALG00000008439	CD36	CD36 molecule	0.87	n.s.

 doi:10.20944/preprints201906.0194.v1

ENSGALG00000046316	CFAP97D1	CFAP97 domain containing 1	1.14	n.s.
ENSGALG00000027874	CHAC1	ChaC glutathione specific gamma-glutamylcyclotransferase 1	1.99	n.s.
ENSGALG00000037856	CHL1	Cell adhesion molecule L1 like	1.44	n.s.
ENSGALG00000034500	CIDEA	Cell death-inducing DFFA-like effector a	1.51	1.22
ENSGALG00000012790	DSP	Desmoplakin	1.50	n.s.
ENSGALG00000015876	ELOVL4	ELOVL fatty acid elongase 4	2.19	n.s.
ENSGALG00000001204	ENKD1	Enkurin domain containing 1	2.07	n.s.
ENSGALG00000008563	ENTPD6	Ectonucleoside triphosphate diphosphohydrolase 6	0.80	n.s.
ENSGALG00000037050	FABP3	Fatty acid binding protein 3	0.77	0.72
ENSGALG00000030025	FABP4	Fatty acid binding protein 4	1.74	1.52
ENSGALG00000013100	GRB10	Growth factor receptor bound protein 10	0.77	n.s.
ENSGALG00000011404	HOPX	HOP homeobox	1.19	1.04
ENSGALG00000023818	HSPB9	Heat shock protein family B (small) member 9	1.14	1.13
ENSGALG00000032672	KRT5	Keratin 5	n.s.	1.68
ENSGALG00000016174	LMBRD1	LMBR1 domain containing 1	0.87	n.s.
ENSGALG00000008805	LMOD2	Leiomodin 2	1.39	n.s.
ENSGALG00000021286	LOC427654	Parvalbumin beta-like	2.36	2.36
ENSGALG00000023819	LOC772158	Heat shock protein 30C-like	0.74	0.76
ENSGALG00000015425	LPL	Lipoprotein lipase	0.80	n.s.
ENSGALG00000043582	LY6CLEL	Lymphocyte antigen 6 complex, locus E-like	2.25	n.s.
ENSGALG00000036004	MRPL34	Mitochondrial ribosomal protein L34	n.s.	0.82
ENSGALG00000001709	MUSTN1	Musculoskeletal, embryonic nuclear protein 1	n.s.	1.30
ENSGALG00000012783	MYBPC1	Myosin binding protein C, slow type	1.49	1.17
ENSGALG00000003323	NECAB2	N-terminal EF-hand calcium binding protein 2	n.s.	1.10
ENSGALG00000053246*	OCM2	Oncomodulin 2	0.78	n.s.
ENSGALG00000013414	PDLIM3	PDZ and LIM domain 3	0.75	n.s.
ENSGALG00000027207	PERP2	PERP2, TP53 apoptosis effector	1.29	n.s.
ENSGALG00000004974	PPARG	Peroxisome proliferator-activated receptor gamma	0.89	n.s.
ENSGALG00000040434	RAB18L	Ras-related protein Rab-18-B-like	1.23	1.09
ENSGALG00000043694	RAPGEF4	Rap guanine nucleotide exchange factor 4	1.24	n.s.
ENSGALG00000002637	RBP7	Retinol binding protein 7	1.96	1.65
ENSGALG00000025650	RF00009	Ribonuclease P RNA component H1, 2 pseudogene	n.s.	0.75
ENSGALG00000051839	RF00012	-	n.s.	2.02
ENSGALG00000047347*	RF00017	-	1.38	n.s.
ENSGALG00000025557	RF00030	-	n.s.	0.88
ENSGALG00000054841*	RF0017	-	0.83	1.46
ENSGALG00000005140	RRAD	RRAD, Ras related glycolysis inhibitor and calcium channel regulator	1.63	1.20
ENSGALG00000051456	RTN2	Reticulon 2	n.s.	1.00
ENSGALG00000009400	SLC8A3	Solute carrier family 8 member A3	0.70	n.s.
ENSGALG00000042863	SMIM4	Small integral membrane protein 4	n.s.	0.87
ENSGALG00000019157	SMPX	Small muscle protein X-linked	0.94	n.s.
ENSGALG00000009037	SPTLC3	Serine palmitoyltransferase long chain base subunit 3	2.47	n.s.
ENSGALG00000031117	STK17A	Serine/threonine kinase 17a	0.92	n.s.
ENSGALG00000021231	TMEM254	Transmembrane protein 254	1.05	n.s.
ENSGALG00000014261	UCHL1	Ubiquitin C-terminal hydrolase L1	1.07	0.94
		Genes downregulated in affected group		
ENSGALG00000025945*	AVD	Avidin	-1.58	-1.69
ENSGALG00000033932	BF1	MHC BF1 class I	-0.84	n.s.
ENSGALG00000006681	BRSK2	BR serine/threonine kinase 2	-2.50	-2.77
ENSGALG00000032220	ELN	Elastin	n.s.	-1.17
ENSGALG00000035309	HBE	Hemoglobin subunit epsilon	-1.59	n.s.

Preprints (www.preprints.org) | NOT PEER-REVIEWED | Posted: 20 June 2019 doi:10.20944/preprints201906.0194.v1

ENSGALG00000002708	LINGO1	Leucine-rich repeat and immunoglobulin-like domain-containing nogo receptor-interacting protein 1	-0.78	-0.77
ENSGALG00000006520	MYH11	Myosin, heavy chain 11, smooth muscle	-0.95	n.s.
ENSGALG00000013045	TUBA8B	Tubulin, alpha 8b	-1.67	n.s.

* These genes had annotation differences between Gallus_gallus-5.0 and GRCg6a reference genome assemblies.

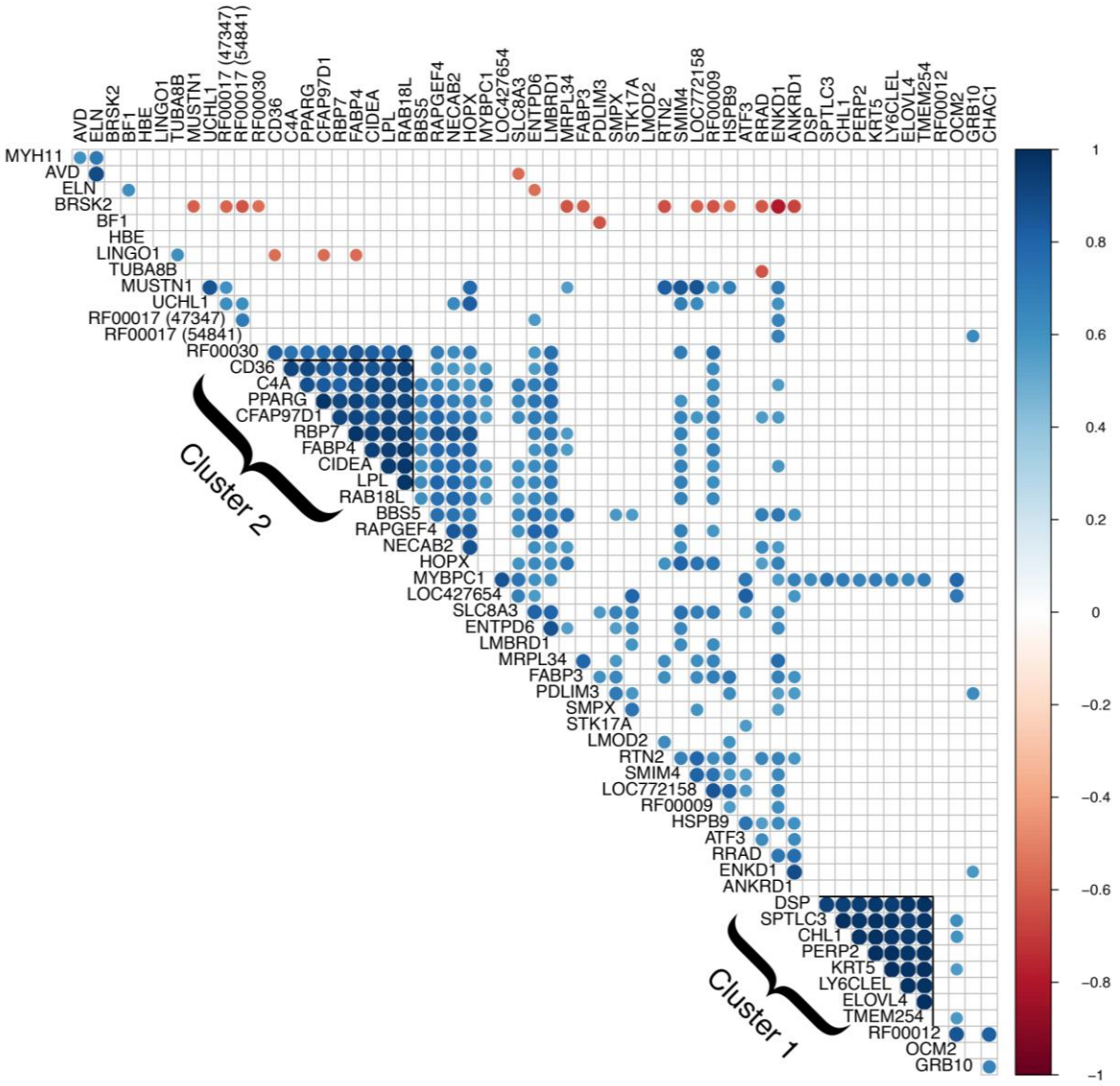

Figure 1. Correlation analysis of differentially expressed genes. Genes with significantly correlated expression (p value ≤ 0.05) are shown in blue (positive correlation) and red (negative correlation). Two major clusters of genes have Pearson's correlation coefficients greater than 0.8 for all gene pairs. Cluster 1 consists of 8 genes, all of which were excluded from further analysis due to presumed skin contamination. Cluster 2 consists of 9 genes related to lipid metabolism or adiposity traits.

Correlation analysis of differentially expressed genes revealed two major clusters with Pearson's correlation coefficients greater than 0.8 for all gene pairs (see Figure 1). The first is a cluster of 8 genes, all of which were excluded from further analysis due to presumed skin contamination. These include *serine palmitoyltransferase long chain base subunit 3* (*SPTLC3*), *desmoplakin* (*DSP*), *ELOVL fatty acid elongase 4* (*ELOVL4*), *PERP2, TP53 apoptosis effector* (*PERP2*), *keratin 5* (*KRT5*), *cell adhesion molecule L1* like (*CHL1*), *lymphocyte antigen 6 complex, locus E-like* (*LY6CLEL*), and *transmembrane protein 254* (*TMEM254*). Several of these genes are known to be primarily expressed in the skin and a previous biopsy study using the same technique demonstrated that biopsy samples are prone to skin

 doi:10.20944/preprints201906.0194.v1

contamination [13]. Additionally, differential expression of these genes was driven by the same three samples, one unaffected and two affected, and expression in the remaining samples was relatively very low or approximately zero. The second cluster consisted of 9 protein-coding genes with demonstrated or putative involvement in lipid metabolism. Although no other clusters were apparent from correlation analysis, functional groupings of differentially expressed genes included muscle growth and function, calcium signaling, and endoplasmic reticulum stress response. We also found a substantial number of genes that are differentially expressed, implicated, or otherwise involved in metabolic syndrome in mammals, which is characterized primarily by diabetes, insulin resistance, obesity, elevated blood lipids, and high blood pressure.

4. Discussion

Metabolic syndrome refers to a cluster of conditions, such as obesity, high blood sugar, high serum triglycerides, low serum HDL cholesterol, and high blood pressure, that put an individual at greater risk of developing type 2 diabetes, atherosclerosis, cardiomyopathy, non-alcoholic fatty liver disease, diabetic nephropathy, and other related disorders. Our data revealed a surprising number of differentially expressed genes implicated in or associated with metabolic syndrome in humans. Among the 60 differentially expressed genes identified in this study, 19 are previously reported to exhibit altered expression in relation to diabetes or a closely related metabolic condition and 10 genes have been identified as candidate genes in association studies of glucose tolerance or diabetes mellitus (Table 2). Two of these candidate genes are associated with diseases that strongly predispose individuals to diabetes and other metabolic complications: a deletion in the elastin gene (ELN) is associated with Williams-Beuren syndrome [20] and mutations in Bardet-Biedl syndrome 5 (BBS5) are associated with Bardet-Biedl Syndrome [21]. Upon further examination, we found that many of the conditions surrounding metabolic syndrome in humans possessed important similarities to the wooden breast phenotype, namely inflammation, ectopic fat deposition, dysregulation of Ca^{2+} homeostasis, endoplasmic reticulum stress, oxidative stress, altered glucose metabolism, fibrosis, and hypertrophy.

Table 2. Differentially expressed genes linked to diabetes and glucose tolerance. Of the 60 differentially expressed genes identified in this study, 26 are either proposed as candidate genes for glucose tolerance or diabetes mellitus or exhibit altered expression in relation to diabetes or a closely related metabolic condition.

Gene Symbol	Gene Name	Connection	Sources
ATF3	Activating transcription factor 3	Expression	[22]
BBS5	Bardet-Biedl syndrome 5	Genetic variant	[21]
BF1	MHC BF1 class I	Expression	[23]
BRSK2	BR serine/threonine kinase 2	Expression	[24]
C4A	Complement C4A (Rodgers blood group)	Expression	[25]
C4A	Complement C4A (Rodgers blood group)	Genetic variant	[24]
CD36	CD36 molecule	Expression	[26,27]
CIDEA	Cell death-inducing DFFA-like effector a	Expression	[28]
ELN	Elastin	Genetic variant	[20]
ENTPD6	Ectonucleoside triphosphate diphosphohydrolase 6 (putative)	Genetic variant	[29]
FABP3	Fatty acid binding protein 3	Expression	[30]
FABP4	Fatty acid binding protein 4	Expression	[30–32]
GRB10	Growth factor receptor bound protein 10	Expression	[33,34]
LINGO1	Leucine-rich repeat and immunoglobulin-like domain-containing nogo receptor-interacting protein 1	Genetic variant	[35,36]
LMBRD1	LMBR1 domain containing 1	Expression	[27]
LMOD2	Leiomodin 2	Genetic variant	[37]
LPL	Lipoprotein lipase	Expression	[32,38]
LPL	Lipoprotein lipase	Genetic variant	[39]
MRPL34	Mitochondrial ribosomal protein L34	Expression	[40,41]

 doi:10.20944/preprints201906.0194.v1

MYH11	Myosin, heavy chain 11, smooth muscle	Expression	[26]
PDLIM3	PDZ and LIM domain 3	Genetic variant	[37]
PPARG	Peroxisome proliferator-activated receptor gamma	Expression	[32,42]
PPARG	Peroxisome proliferator-activated receptor gamma	Genetic variant	[43–47]
RAB18L	Ras-related protein Rab-18-B-like	Expression	[48]
RAPGEF4	Rap guanine nucleotide exchange factor 4	Expression	[49]
RBP7	Retinol binding protein 7	Expression	[50]
RRAD	RRAD, Ras related glycolysis inhibitor and calcium channel regulator	Expression	[26]
RTN2	Reticulon 2	Genetic variant	[24]
UCHL1	Ubiquitin C-terminal hydrolase L1	Expression	[51]

One of the most compelling links to metabolic syndrome in our data is *RRAD, ras related glycolysis inhibitor and calcium channel regulator* (*RRAD*), a gene originally named *Ras-related associated with diabetes* because it was identified via subtraction cloning as the only gene out of 4000 cDNA clones that was overexpressed in skeletal muscle of type 2 diabetic individuals compared to non-diabetic or type 1 diabetic individuals [26]. RRAD is a small GTPase that binds directly to Ca^{2+} channel beta subunits to regulate intracellular Ca^{2+} signaling in muscle cells [52] and may also have regulatory functions via its interaction with calmodulin [53]. Overexpression of *RRAD* in cultured myocytes was found to reduce insulin-stimulated glucose uptake by 50-90%, which the authors speculated was due to a decrease in intrinsic activity of glucose transporter 4, the insulin-dependent glucose transporter [54]. An in vivo study of transgenic mice overexpressing *RRAD* in skeletal muscle found that high fat feeding produced not only insulin resistance in transgenic mice, but also increased triglyceride metabolism compared to controls [55]. This suggests that RRAD may inhibit glycolysis independently from its action on glucose transporters via substrate competition [56]. Another regulator of intracellular Ca^{2+}, *RAPGEF4*, upregulated in the current study, is the direct target of some anti-diabetic drugs called sulfonylureas [49]. The role of Ca^{2+} in metabolic syndrome is complex and not fully understood, but one theory suggests that the disruption of Ca^{2+} homeostasis is a feed-forward pathological cycle resulting from endoplasmic reticulum dysfunction during chronic exposure to excessive nutrients and energy [57].

Endoplasmic reticulum stress in affected birds is supported in our study by the upregulation of *activating transcription factor 3* (*ATF3*), *ChaC glutathione specific gamma-glutamylcyclotransferase 1* (*CHAC1*), and *reticulon 2* (*RTN2*) and the downregulation of *BR serine/threonine kinase 2* (*BRSK2*). *ATF3*, *CHAC1,* and *BRSK2* are part of the unfolded protein response [58,59], a highly conserved cellular stress response caused by an accumulation of unfolded or misfolded proteins in the endoplasmic reticulum [60]. An association between the unfolded protein response, lipid metabolism, and metabolic syndrome has been clearly established, but the direction of causality is controversial [61–64]. The role of ATF3 in particular has been studied in the context of type 2 diabetes, non-alcoholic fatty liver disease, diabetic cardiomyopathy, atherosclerosis, and obesity, with some authors suggesting it may have both detrimental and beneficial functions related to insulin resistance, mitochondrial dysfunction, and inflammation in response to high fat diets [22,65–71]. In arterial endothelial cells, ATF3 expression can be induced by exposure to high levels of triglyceride-rich lipoprotein lipolysis products [66], substantiating it as a link between high lipid metabolism and cellular stress response.

Ectopic lipid deposition and the resulting lipotoxicity are considered to be a major cause of metabolic syndrome with the precise location of ectopic lipid accumulation dictating specific complications such as atherosclerosis, hepatic steatosis, and diabetic nephropathy [72]. Our results strongly support increased lipid metabolism in the pectoralis major of affected birds. Many of the differentially expressed genes from our analysis encode proteins with critical or rate-limiting functions in lipid metabolism and homeostasis such as lipoprotein triglyceride hydrolysis, fatty acid transport, and lipid droplet regulation. These genes include *lipoprotein lipase* (*LPL*), *CD36 molecule* (*CD36*), *peroxisome proliferator-activated receptor gamma* (*PPARG*), *retinol binding protein 7* (*RBP7*), *fatty acid binding protein 3* (FABP3), fatty *acid binding protein 4* (*FABP4*), *cell death-inducing DFFA-like effector a* (*CIDEA*), *ras-related protein Rab-18-B-like* (*RAB18L*), and *LMBR1 domain containing 1* (*LMBRD1*)

 doi:10.20944/preprints201906.0194.v1

[31,48,73–81]. Several other genes, some of which are functionally uncharacterized or poorly understood with regard to lipid metabolism, have expression or genetic polymorphisms correlated with adiposity traits such as body mass index, percent intramuscular fat, percent abdominal fat, or blood lipid levels. These genes include *HOP homeobox* (*HOPX*), *myosin binding protein C, slow type* (*MYBPC1*), and *Bardet-Biedl syndrome 5* (*BBS5*), *growth factor receptor bound protein 10* (*GRB10*), *CFAP97 domain containing 1* (*CFAP97D1*), *hemoglobin subunit epsilon* (*HBE*), *ectonucleoside triphosphate diphosphohydrolase 6* (ENTPD6), *complement C4A (Rodgers blood group)* (*C4A*), *mitochondrial ribosomal protein L34* (*MRPL34*), *ATF3*, and *CHAC1* [67,82–95]. This evidence of increased lipid metabolism and fat deposition in the pectoralis major is consistent with histological examinations of 2-week-old birds with wooden breast, in which lipid infiltration and accumulation was established as one of the first signs of disease [2].

A large cluster of upregulated genes related to lipid metabolism from the present study were found to exhibit highly correlated expression with Pearson's correlation coefficients greater than 0.8 for all gene pairs (see Figure 1). We believe this cluster may represent a functional group as it includes the transcription factor PPARγ and several of its experimentally validated transcriptional targets (*CD36*, *C4A*, *RBP7*, *FABP4*, *CIDEA*, and *LPL*) [77,78,82,96,97]. Upregulation of PPARγ in the early stages of wooden breast is especially important because, as a master regulator of adipogenesis, it is a critical component in governing the distribution of lipid deposition in the body and the development of various metabolic conditions [98–102]. It is also one of the few established genes that has been associated with common forms of type 2 diabetes across multiple genome-wide association studies [43–47]. While PPARγ is mainly associated with adipose tissue [97], it possesses important functions in skeletal muscle and other tissues. A knockout study in mice found that PPARγ is not only critical for fat infiltration during skeletal muscle regeneration, but that it is required for muscle stem cell function and efficient muscle repair due to crosstalk with two myogenic transcription factors, myogenic differentiation 1 (MYOD1) and paired box 7 (PAX7) [103]. In skeletal muscle of broiler chickens and other meat-type animals, increased expression of *PPARG* and PPARγ target genes is frequently associated with higher intramuscular fat content [104–107].

Several genes involved in myogenic differentiation and muscle hypertrophy are upregulated in affected birds: *musculoskeletal, embryonic nuclear protein 1* (*MUSTN1*), *ankyrin repeat domain 1* (*ANKRD1*), and *HOPX* have roles in myotube formation, myofusion, and regulation of other myoblast differentiation genes [85,108–112], although studies of *HOPX* in chickens have found that it's highly expressed in adipose tissue and has functions related to adipocyte differentiation [84,85]. Other upregulated genes related to development and regeneration of the musculosketal system include *PDZ and LIM domain 3* (*PDLIM3*), *small muscle protein X-linked* (*SMPX*), and *leiomodin 2* (*LMOD2*). Two of these, *SMPX* and *PDLIM3*, encode Z-disc associated proteins with putative mechanosensory or stretch signaling roles in striated muscle [113,114]. Expression of *MUSTN1*, *ANKRD1*, *PDLIM3*, and *SMPX* can be induced by eccentric contraction exercises [115–117] or passive stretch [118], suggesting a role in muscle hypertrophy and repair [114]. Upregulation of genes related to hypertrophy in affected birds is in line with higher breast muscle yield in affected birds [4,6,7]. In fact, speculation on the cause of wooden breast and related muscle disorders has focused largely on impaired oxygen supply and buildup of metabolic waste resulting from sustained rapid growth of the pectoralis major [8,119–121]. However, upregulation of these genes may also be part of the disease progression. If wooden breast is a metabolic disorder with similarities to diabetes, e.g. in dysregulation of intracellular calcium homeostasis [12,13] and intracellular glucose metabolism [14], excessive growth of the pectoralis major in affected chickens might be, at least in part, a symptom of the disease rather than solely a predisposing factor. Although diabetes generally causes skeletal muscle atrophy, various complications of diabetes such as cardiomyopathy, non-alcoholic fatty liver disease, and diabetic nephropathy can cause structural remodeling that includes hypertrophy and even fibrosis of the of the heart, liver, and kidneys respectively [122–124].

Interestingly, our data showed upregulation of several genes, such as *MYBPC1* and *SMPX* [125,126], that are more closely associated with slow-twitch oxidative muscle rather than fast-twitch glycolytic muscle. For example, *LMOD2* has been alternatively called cardiac leiomodin and its levels

in cardiac muscle are directly linked to the length of actin-containing thin filaments due to competition for binding with tropomodulin-1 [127]. Overexpression of *LMOD2* in the heart results in elongation of thin filaments and reduced cardiac function as proper thin filament length is necessary to generate contractile force [127,128]. Similarly, *ANKRD1* was previously named cardiac ankyrin repeat protein (CARP) and has been proposed as a marker of cardiac hypertrophy due to its increased expression in 3 distinct models of cardiac hypertrophy in rats [129]. The lipid transporter *FABP3*, which is involved in the uptake, intracellular metabolism and transport of long-chain fatty acids, is most abundantly expressed in slow-twitch skeletal and cardiac muscle of humans [93]. Upregulation of these genes is consistent with previous reports of fiber-type switching in 7-week-old birds with wooden breast [12] and may suggest that the pectoralis major muscle of affected birds resembles cardiac or slow-twitch muscle at the transcriptional level despite the metabolic limitations of glycolytic muscle fibers.

5. Conclusions

The findings of this study show that transcriptional changes associated with early stages of wooden breast disease in 2-week-old birds have significant overlap with genes that are dysregulated in metabolic syndrome in humans. Although the underlying causes of metabolic dysfunction possibly leading to pathological progression of the disease remain unknown, this study clearly demonstrates that early upregulation of lipid metabolism in the pectoralis major is a key feature of the myopathy. Affected birds also show dysregulation of various genes involved in muscle growth and function as well as calcium signaling and endoplasmic reticulum stress. Our results are consistent with previous reports of metabolic perturbations in wooden breast [12–14], especially a recent study suggesting that the increased ability to direct alimentary resources, particularly fatty acids, to the pectoralis major muscle may underlie susceptibility to wooden breast [5]. Additional studies are needed to understand the mechanisms underlying this metabolic dysfunction and to investigate the possible link between wooden breast and metabolic syndrome.

Supplementary Materials: The following are available online at www.mdpi.com/xxx/s1, Table S1: Sequencing and mapping statistics for RNA-Seq analysis of 8 wooden breast affected and 6 unaffected pectoralis major muscle samples.

Author Contributions: Conceptualization, Juniper A. Lake and Behnam Abasht; Formal analysis, Juniper A. Lake; Funding acquisition, Behnam Abasht; Investigation, Juniper A. Lake and Behnam Abasht; Methodology, Juniper A. Lake, Michael B. Papah and Behnam Abasht; Project administration, Behnam Abasht; Resources, Behnam Abasht; Software, Juniper A. Lake; Supervision, Behnam Abasht; Validation, Juniper A. Lake and Behnam Abasht; Visualization, Juniper A. Lake; Writing – original draft, Juniper A. Lake; Writing – review & editing, Michael B. Papah and Behnam Abasht.

Funding: This research was funded by the U.S. Department of Agriculture, Agriculture and Food Research Initiative competitive grant number 2016-67015-25027.

Acknowledgments: The authors gratefully acknowledge the in-kind support by Cobb-Vantress Inc. in providing chicks and chicken feed for this experiment. We also greatly appreciate assistance with samples and data collection from many graduate and undergraduate students at the University of Delaware Department of Animal and Food Sciences. We would like to acknowledge the support from the University of Delaware Center for Bioinformatics and Computational Biology for utilization of their cluster BioMix, which was made possible through support from the Delaware INBRE (NIH GM103446), the state of Delaware and the Delaware Biotechnology Institute (DBI). RNA sequencing services at DBI are greatly appreciated.

Conflicts of Interest: The authors declare no conflict of interest.

References

1. Gall, S.; Suyemoto, M.M.; Sather, H.M.L.; Sharpton, A.R.; Barnes, H.J.; Borst, L.B. Wooden breast in commercial broilers associated with mortality, dorsal recumbency, and pulmonary disease. *Avian Dis. In-Press* **2019**.

2. Papah, M.B.; Brannick, E.M.; Schmidt, C.J.; Abasht, B. Evidence and role of phlebitis and lipid infiltration in the onset and pathogenesis of Wooden Breast Disease in modern broiler chickens. *Avian Pathol.* **2017**, *46*, 623–643.
3. Norring, M.; Valros, A.; Valaja, J.; Sihvo, H.; Immonen, K.; Puolanne, E. Wooden breast myopathy links with poorer gait in broiler chickens. *Animal* **2018**, 1–6.
4. Mutryn, M.F.; Fu, W.; Abasht, B. Incidence of Wooden Breast Disease and its correlation with broiler performance and ultimate pH of breast muscle. In Proceedings of the Proceedings of XXII European Symposium on Poultry Meat Quality; Nantes, France, 2015.
5. Abasht, B.; Zhou, N.; Lee, W.R.; Zhuo, Z.; Peripolli, E. The metabolic characteristics of susceptibility to wooden breast disease in chickens with high feed efficiency. *Poult. Sci.* **2019**, 1–11.
6. Dalle Zotte, A.; Cecchinato, M.; Quartesan, A.; Bradanovic, J.; Puolanne, E. How does "Wooden Breast" myodegradation affect poultry meat quality? In Proceedings of the 60th International Congress of Meat Science and Technology; Punta Del Este, Uruguay, 2014.
7. Bailey, R.A.; Watson, K.A.; Bilgili, S.F.; Avendano, S. The genetic basis of pectoralis major myopathies in modern broiler chicken lines. *Poult. Sci.* **2015**, *94*, 2870–2879.
8. Mudalal, S.; Lorenzi, M.; Soglia, F.; Cavani, C.; Petracci, M. Implications of white striping and wooden breast abnormalities on quality traits of raw and marinated chicken meat. *Animal* **2015**, *9*, 728–734.
9. Trocino, A.; Piccirillo, A.; Birolo, M.; Radaelli, G.; Bertotto, D.; Filiou, E.; Petracci, M.; Xiccato, G. Effect of genotype, gender and feed restriction on growth, meat quality and the occurrence of white striping and wooden breast in broiler chickens. *Poult. Sci.* **2015**, *94*, 2996–3004.
10. Livingston, M.L.; Ferket, P.R.; Brake, J.; Livingston, K.A. Dietary amino acids under hypoxic conditions exacerbates muscle myopathies including wooden breast and white stripping. *Poult. Sci.* **2019**, *98*, 1517–1527.
11. Sihvo, H.K.; Immonen, K.; Puolanne, E. Myodegeneration with fibrosis and regeneration in the pectoralis major muscle of broilers. *Vet. Pathol.* **2014**, *51*, 619–623.
12. Mutryn, M.F.; Brannick, E.M.; Fu, W.; Lee, W.R.; Abasht, B. Characterization of a novel chicken muscle disorder through differential gene expression and pathway analysis using RNA-sequencing. *BMC Genomics* **2015**, *16*, 1–19.
13. Papah, M.B.; Brannick, E.M.; Schmidt, C.J.; Abasht, B. Gene expression profiling of the early pathogenesis of wooden breast disease in commercial broiler chickens using RNA-sequencing. *PLoS One* **2018**, *13*, e0207346.
14. Abasht, B.; Mutryn, M.F.; Michalek, R.D.; Lee, W.R. Oxidative stress and metabolic perturbations in wooden breast disorder in chickens. *PLoS One* **2016**, *11*, 1–16.
15. FastQC Available online: https://www.bioinformatics.babraham.ac.uk/projects/fastqc/.
16. Bolger, A.M.; Lohse, M.; Usadel, B. Trimmomatic: A flexible trimmer for Illumina sequence data. *Bioinformatics* **2014**, *30*, 2114–2120.
17. Kim, D.; Langmead, B.; Salzberg, S.L. HISAT: A fast spliced aligner with low memory requirements. *Nat. Methods* **2015**, *12*, 357–360.
18. Trapnell, C.; Hendrickson, D.G.; Sauvageau, M.; Goff, L.; Rinn, J.L.; Pachter, L. Differential analysis of gene regulation at transcript resolution with RNA-seq. *Nat. Biotechnol.* **2013**, *31*, 46–53.
19. Wei, T.; Simko, V. R package "corrplot": Visualization of a correlation matrix (Version 0.84) 2017.
20. DeMarsilis, A.J.; Walji, T.A.; Maedeker, J.A.; Stoka, K. V; Kozel, B.A.; Mecham, R.P.; Wagenseil, J.E.; Craft, C.S. Elastin insufficiency predisposes mice to impaired glucose metabolism. *J. Mol. Genet. Med.*

2014, *8*, 1247–1262.

21. Beales, P.L.; Elcioglu, N.; Woolf, A.S.; Parker, D.; Flinter, F.A. New criteria for improved diagnosis of Bardet-Biedl syndrome: results of a population survey. *J. Med. Genet.* **1999**, *36*, 437–46.
22. Qi, L.; Saberi, M.; Zmuda, E.; Wang, Y.; Altarejos, J.; Zhang, X.; Dentin, R.; Hedrick, S.; Bandyopadhyay, G.; Hai, T.; et al. Adipocyte CREB promotes insulin resistance in obesity. *Cell Metab.* **2009**, *9*, 277–286.
23. Faustman, D.; Li, X.; Lin, H.Y.; Fu, Y.; Eisenbarth, G.; Avruch, J.; Guo, J. Linkage of faulty major histocompatibility complex class I to autoimmune diabetes. *Science (80-.).* **1991**, *254*, 1756–1761.
24. Caplen, N.J.; Patel, A.; Millward, A.; Campbell, R.D.; Ratanachaiyavong, S.; Wong, F.S.; Demaine, A.G. Complement C4 and heat shock protein 70 (HSP70) genotypes and type I diabetes mellitus. *Immunogenetics* **1990**, *32*, 427–430.
25. Lappas, M. Lower circulating levels of complement split proteins C3a and C4a in maternal plasma of women with gestational diabetes mellitus. *Diabet. Med.* **2011**, *28*, 906–911.
26. Reynet, C.; Kahn, C.R. Rad: A member of the Ras family overexpressed in muscle of type II diabetic humans. *Science (80-.).* **1993**, *262*, 1441.
27. Tan, A.L.M.; Langley, S.R.; Tan, C.F.; Chai, J.F.; Khoo, C.M.; Leow, M.K.S.; Khoo, E.Y.H.; Moreno-Moral, A.; Pravenec, M.; Rotival, M.; et al. Ethnicity-specific skeletal muscle transcriptional signatures and their relevance to insulin resistance in Singapore. *J. Clin. Endocrinol. Metab.* **2018**, *104*, 465–486.
28. Zhou, L.; Xu, L.; Ye, J.; Li, D.; Wang, W.; Li, X.; Wu, L.; Wang, H.; Guan, F.; Li, P. Cidea promotes hepatic steatosis by sensing dietary fatty acids. *Hepatology* **2012**, *56*, 95–107.
29. Rich, S.S.; Goodarzi, M.O.; Palmer, N.D.; Langefeld, C.D.; Ziegler, J.; Haffner, S.M.; Bryer-Ash, M.; Norris, J.M.; Taylor, K.D.; Haritunians, T.; et al. A genome-wide association scan for acute insulin response to glucose in Hispanic-Americans: The Insulin Resistance Atherosclerosis Family Study (IRAS FS). *Diabetologia* **2009**, *52*, 1326–1333.
30. Husi, H.; Van Agtmael, T.; Mullen, W.; Bahlmann, F.H.; Schanstra, J.P.; Vlahou, A.; Delles, C.; Perco, P.; Mischak, H. Proteome-based systems biology analysis of the diabetic mouse aorta reveals major changes in fatty acid biosynthesis as potential hallmark in diabetes mellitus-associated vascular disease. *Circ. Cardiovasc. Genet.* **2014**, *7*, 161–170.
31. Furuhashi, M.; Saitoh, S.; Shimamoto, K.; Miura, T. Fatty acid-binding protein 4 (FABP4): Pathophysiological insights and potent clinical biomarker of metabolic and cardiovascular diseases. *Clin. Med. Insights Cardiol.* **2014**, *2014*, 23–33.
32. Westerbacka, J.; Kolak, M.; Kiviluoto, T.; Arkkila, P.; Sire, J.; Hamsten, A.; Fisher, R.M.; Yki-ja, H. Genes involved in fatty acid partitioning and binding, inflammation are overexpressed in the human fatty liver of insulin-resistant subjects. *Diabetes* **2007**, *56*, 2759–2765.
33. Lim, M.A.; Riedel, H.; Liu, F. Grb10: more than a simple adaptor protein. *Front. Biosci.* **2007**, *9*, 387–403.
34. Yang, S.; Deng, H.; Zhang, Q.; Xie, J.; Zeng, H.; Jin, X.; Ling, Z.; Shan, Q.; Liu, M.; Ma, Y.; et al. Amelioration of diabetic mouse nephropathy by catalpol correlates with down-regulation of Grb10 adn activation of insulin-like growth factor 1/insulin-like growth factor 1 receptor signaling. *PLoS One* **2016**, *11*, e0151857.
35. Abdullah, N.; Abdul Murad, N.A.; Attia, J.; Oldmeadow, C.; Mohd Haniff, E.A.; Syafruddin, S.E.; Abd Jalal, N.; Ismail, N.; Ishak, M.; Jamal, R.; et al. Characterizing the genetic risk for Type 2 diabetes in a Malaysian multi-ethnic cohort. *Diabet. Med.* **2015**, *32*, 1377–1384.
36. Morris, A.D.P.; Voight, B.F.; Teslovich, T.M.; Ferreira, T.; Segrè, A. V.; Steinthorsdottir, V.; Strawbridge, R.J.; Khan, H.; Grallert, H.; Mahajan, A.; et al. Large-scale association analysis provides insights into the

genetic architecture and pathophysiology of type 2 diabetes. *Nat. Genet.* **2012**, *44*, 981–990.

37. Kang, H.P.; Yang, X.; Chen, R.; Zhang, B.; Corona, E.; Schadt, E.E.; Butte, A.J. Integration of disease-specific single nucleotide polymorphisms, Expression quantitative trait loci and coexpression networks reveal novel candidate genes for type 2 diabetes. *Diabetologia* **2012**, *55*, 2205–2213.
38. Howard, B. V. Lipoprotein metabolism in diabetes mellitus. *J. Lipid Res.* **1987**, *28*, 613–628.
39. Yang, T.; Pang, C.P.; Tsang, M.W.; Lam, C.W.; Poon, P.M.K.; Chan, L.Y.S.; Wu, X.Q.; Tomlinson, B.; Baum, L. Pathogenic mutations of the lipoprotein lipase gene in Chinese patients with hypertriglyceridemic type 2 diabetes. *Hum. Mutat.* **2003**, *21*, 453.
40. Park, P.J.; Kong, S.W.; Tebaldi, T.; Lai, W.R.; Kasif, S.; Kohane, I.S. Integration of heterogeneous expression data sets extends the role of the retinol pathway in diabetes and insulin resistance. *Bioinformatics* **2009**, *25*, 3121–3127.
41. Moreno-Viedma, V.; Amor, M.; Sarabi, A.; Bilban, M.; Staffler, G.; Zeyda, M.; Stulnig, T.M. Common dysregulated pathways in obese adipose tissue and atherosclerosis. *Cardiovasc. Diabetol.* **2016**, *15*, 1–12.
42. Park, K.S.; Ciaraldi, T.P.; Abrams-carter, L.; Mudaliar, S.; Nikoulina, S.E.; Henry, R.R. PPAR-y gene expression is elevated in skeletal muscle of obese and type II diabetic subjects. *Diabetes* **1997**, *46*, 1230–1234.
43. Zeggini, E.; Scott, L.J.; Saxena, R.; Voight, B.F. Meta-analysis of genome-wide association data and large-scale replication identifies additional susceptibility loci for type 2 diabetes. *Nat. Genet.* **2008**, *40*, 638–645.
44. Scott, L.J.; Mohlke, K.L.; Bonnycastle, L.L.; Willer, C.J.; Li, Y.; Duren, W.L.; Erdos, M.R.; Stringham, H.M.; Chines, P.S.; Jackson, A.U.; et al. A genome-wide association study of type 2 diabetes in finns detects multiple susceptibility variants. *Science (80-.).* **2007**, *316*, 1341–1345.
45. Sanghera, D.K.; Blackett, P.R. Type 2 diabetes genetics: Beyond GWAS. *J. Diabetes Metab.* **2012**, *3*, 6948.
46. Sladek, R.; Rocheleau, G.; Rung, J.; Dina, C.; Shen, L.; Serre, D.; Boutin, P.; Vincent, D.; Belisle, A.; Hadjadj, S.; et al. A genome-wide association study identifies novel risk loci for type 2 diabetes. *Nature* **2007**, *445*, 881–885.
47. Stumvoll, M.; Häring, H. The peroxisome proliferator–activated receptor-gamma2 Pro12Ala polymorphism. *Diabetes* **2002**, *51*, 2341–2347.
48. Pulido, M.R.; Diaz-Ruiz, A.; Jiménez-Gómez, Y.; Garcia-Navarro, S.; Gracia-Navarro, F.; Tinahones, F.; López-Miranda, J.; Frühbeck, G.; Vázquez-Martínez, R.; Malagón, M.M. Rab18 dynamics in adipocytes in relation to lipogenesis, lipolysis and obesity. *PLoS One* **2011**, *6*.
49. Zhang, C.-L.; Katoh, M.; Shibasaki, T.; Minami, K.; Sunaga, Y.; Takahashi, H.; Yokoi, N.; Iwasaki, M.; Miki, T.; Susumu, S. The cAMP sensor Epac2 is a direct target of antidiabetic sulfonylurea drugs. *Science* **2009**, *325*, 607–610.
50. Nie, J.; DuBois, D.C.; Xue, B.; Jusko, W.J.; Almon, R.R. Effects of high-fat feeding on skeletal muscle gene expression in diabetic Goto-Kakizaki rats. *Gene Regul. Syst. Bio.* **2017**, *11*, 1–11.
51. Zhang, H.; Luo, W.; Sun, Y.; Qiao, Y.; Zhang, L.; Zhao, Z.; Lv, S. Wnt/β-catenin signaling mediated-UCH-L1 expression in podocytes of diabetic nephropathy. *Int. J. Mol. Sci.* **2016**, *17*.
52. Finlin, B.S.; Crump, S.M.; Satin, J.; Andres, D.A. Regulation of voltage-gated calcium channel activity by the Rem and Rad GTPases. *Proc. Natl. Acad. Sci. U. S. A.* **2003**, *100*, 14469–74.
53. Moyers, J.S.; Bilan, P.J.; Zhu, J.; Kahn, C.R. Rad and Rad-related GTPases interact with calmodulin and calmodulin- dependent protein kinase II. *J. Biol. Chem.* **1997**, *272*, 11832–11839.
54. Moyers, J.S.; Bilan, P.J.; Reynet, C.; Ronald Kahn, C. Overexpression of Rad inhibits glucose uptake in cultured muscle and fat cells. *J. Biol. Chem.* **1996**, *271*, 23111–23116.

55. Ilany, J.; Bilan, P.J.; Kapur, S.; Caldwell, J.S.; Patti, M.-E.; Marette, A.; Kahn, C.R. Overexpression of Rad in muscle worsens diet-induced insulin resistance and glucose intolerance and lowers plasma triglyceride level. *Proc. Natl. Acad. Sci.* **2006**, *103*, 4481–4486.
56. Randle, P.J.; Priestman, D.A.; Mistry, S.C.; Halsall, A. Glucose fatty acid interactions and the regulation of glucose disposal. *J. Cell. Biochem.* **1994**, *55*, 1–11.
57. Arruda, A.P.; Hotamisligil, G.S. Calcium homeostasis and organelle function in the pathogenesis of obesity and diabetes. *Cell Metab.* **2015**, *22*, 381–397.
58. Mungrue, I.N.; Pagnon, J.; Kohannim, O.; Gargalovic, P.S.; Lusis, A.J. CHAC1/MGC4504 is a novel proapoptotic component of the unfolded protein response, downstream of the ATF4-ATF3-CHOP cascade. *J. Immunol.* **2009**, *182*, 466–476.
59. Wang, Y.; Wan, B.; Li, D.; Zhou, J.; Li, R.; Bai, M.; Chen, F.; Yu, L. BRSK2 is regulated by ER stress in protein level and involved in ER stress-induced apoptosis. *Biochem. Biophys. Res. Commun.* **2012**, *423*, 813–818.
60. Schröder, M.; Kaufman, R.J. ER stress and the unfolded protein response. *Mutat. Res. - Fundam. Mol. Mech. Mutagen.* **2005**, *569*, 29–63.
61. Volmer, R.; Ron, D. Lipid-dependent regulation of the unfolded protein response. *Curr. Opin. Cell Biol.* **2015**, *33*, 67–73.
62. Eizirik, D.L.; Cardozo, A.K.; Cnop, M. The role for endoplasmic reticulum stress in diabetes mellitus. *Endocr. Rev.* **2008**, *29*, 42–61.
63. Basseri, S.; Austin, R.C. Endoplasmic reticulum stress and lipid metabolism: Mechanisms and therapeutic potential. *Biochem. Res. Int.* **2012**, *2012*.
64. Cnop, M.; Foufelle, F.; Velloso, L.A. Endoplasmic reticulum stress, obesity and diabetes. *Trends Mol. Med.* **2012**, *18*, 59–68.
65. Zmuda, E.J.; Qi, L.; Zhu, M.X.; Mirmira, R.G.; Montminy, M.R.; Hai, T. The roles of ATF3 , an adaptive-response gene, in high-fat-diet-induced diabetes and pancreatic β-cell dysfunction. *Mol. Endocrinol.* **2010**, *24*, 1423–1433.
66. Aung, H.H.; Lame, M.W.; Gohil, K.; An, C. Il; Wilson, D.W.; Rutledge, J.C. Induction of ATF3 gene network by triglyceride-rich lipoprotein lipolysis products increases vascular apoptosis and inflammation. *Arterioscler. Thromb. Vasc. Biol.* **2013**, *33*, 2088–2096.
67. Jang, M.K.; Son, Y.; Jung, M.H. ATF3 plays a role in adipocyte hypoxia-mediated mitochondria dysfunction in obesity. *Biochem. Biophys. Res. Commun.* **2013**, *431*, 421–427.
68. Kalfon, R.; Koren, L.; Aviram, S.; Schwartz, O.; Hai, T.; Aronheim, A. ATF3 expression in cardiomyocytes preserves homeostasis in the heart and controls peripheral glucose tolerance. *Cardiovasc. Res.* **2017**, *113*, 134–146.
69. Kim, J.Y.; Park, K.J.; Hwang, J.Y.; Kim, G.H.; Lee, D.Y.; Lee, Y.J.; Song, E.H.; Yoo, M.G.; Kim, B.J.; Suh, Y.H.; et al. Activating transcription factor 3 is a target molecule linking hepatic steatosis to impaired glucose homeostasis. *J. Hepatol.* **2017**, *67*, 349–359.
70. Kim, S.; Song, N.J.; Bahn, G.; Chang, S.H.; Yun, U.J.; Ku, J.M.; Jo, D.G.; Park, K.W. Atf3 induction is a therapeutic target for obesity and metabolic diseases. *Biochem. Biophys. Res. Commun.* **2018**, *504*, 903–908.
71. Hyun, B.K.; Kong, M.; Tae, M.K.; Young, H.S.; Kim, W.H.; Joo, H.L.; Ji, H.S.; Myeong, H.J. NFATc4 and ATF3 negatively regulate adiponectin gene expression in 3T3-L1 adipocytes. *Diabetes* **2006**, *55*, 1342–1352.
72. Rasouli, N.; Molavi, B.; Elbein, S.C.; Kern, P.A. Ectopic fat accumulation and metabolic syndrome.

Diabetes, Obes. Metab. **2007**, *9*, 1–10.

73. Zerega, B.; Camardella, L.; Cermelli, S.; Sala, R.; Cancedda, R.; Descalzi Cancedda, F. Avidin expression during chick chondrocyte and myoblast development in vitro and in vivo: regulation of cell proliferation. *J Cell Sci* **2001**, *114*, 1473–1482.
74. Mead, J.R.; Irvine, S.A.; Ramji, D.P. Lipoprotein lipase: Structure, function, regulation, and role in disease. *J. Mol. Med.* **2002**, *80*, 753–769.
75. Wang, H.; Eckel, R.H. Lipoprotein lipase: from gene to obesity. *Am. J. Physiol. Metab.* **2009**, *297*, E271–E288.
76. Bonen, A.; Parolin, M.L.; Steinberg, G.R.; Calles-Escandon, J.; Tandon, N.N.; Glatz, J.F.C.; Luiken, J.J.F.P.; Heigenhauser, G.J.F.; Dyck, D.J. Triacylglycerol accumulation in human obesity and type 2 diabetes is associated with increased rates of skeletal muscle fatty acid transport and increased sarcolemmal FAT/CD36. *FASEB J.* **2004**, *18*, 1144–1146.
77. Zizola, C.F.; Schwartz, G.J.; Vogel, S. Cellular retinol-binding protein type III is a PPARγ target gene and plays a role in lipid metabolism. *Am. J. Physiol. Metab.* **2008**, *295*, E1358–E1368.
78. Puri, V.; Ranjit, S.; Konda, S.; Nicoloro, S.M.C.; Straubhaar, J.; Chawla, A.; Chouinard, M.; Lin, C.; Burkart, A.; Corvera, S.; et al. Cidea is associated with lipid droplets and insulin sensitivity in humans. *Proc. Natl. Acad. Sci.* **2008**, *105*, 7833–7838.
79. Martin, S.; Parton, R.G. Characterization of Rab18, a lipid droplet-associated Small GTPase. In *Methods in Enzymology*; 2008; Vol. 438, pp. 109–129 ISBN 9780123739681.
80. Green, C.R.; Wallace, M.; Divakaruni, A.S.; Phillips, S.A.; Murphy, A.N.; Ciaraldi, T.P.; Metallo, C.M. Branched-chain amino acid catabolism fuels adipocyte differentiation and lipogenesis. *Nat. Chem. Biol.* **2016**, *12*, 15–21.
81. Rutsch, F.; Gailus, S.; Suormala, T.; Fowler, B. LMBRD1: The gene for the cblF defect of vitamin B12 metabolism. *J. Inherit. Metab. Dis.* **2011**, *34*, 121–126.
82. Szatmari, I.; Töröcsik, D.; Agostini, M.; Nagy, T.; Gurnell, M.; Barta, E.; Chatterjee, K.; Nagy, L. PPARγ regulates the function of human dendritic cells primarily by altering lipid metabolism. *Blood* **2007**, *110*, 3271–3280.
83. Turcot, V.; Lu, Y.; Highland, H.M.; Schurmann, C.; Justice, A.E.; Fine, R.S.; Bradfield, J.P.; Esko, T.; Giri, A.; Graff, M.; et al. Protein-altering variants associated with body mass index implicate pathways that control energy intake and expenditure in obesity. *Nat. Genet.* **2018**, *50*, 26–35.
84. Hong-yan, S.H.I.; Qi, H.E.; Min, C.; Ying-ning, S.U.N.; Hui, L.I.; Ning, W. Effect of HOPX gene overexpression on chicken preadipocyte proliferation. **2015**, *48*, 1624–1631.
85. Zhang, K.; Zhang, Z.W.; Wang, W.S.; Yan, X.H.; Li, H.; Wang, N. Cloning and expression of chicken HOPX gene. *J. Northeast Agric. Univ.* **2012**, *43*, 46–53.
86. Chen, Z.; Zhao, T.-J.; Li, J.; Gao, Y.-S.; Meng, F.-G.; Yan, Y.-B.; Zhou, H.-M. Slow skeletal muscle myosin-binding protein-C (MyBPC1) mediates recruitment of muscle-type creatine kinase (CK) to myosin. *Biochem. J.* **2011**, *436*, 437–445.
87. Liu, M.; Bai, J.; He, S.; Villarreal, R.; Hu, D.; Zhang, C.; Yang, X.; Liang, H.; Slaga, T.J.; Yu, Y.; et al. Grb10 promotes lipolysis and thermogenesis by phosphorylation-dependent feedback inhibition of mTORC1. *Cell Metab.* **2014**, *19*, 967–980.
88. Van Leeuwen, E.M.; Karssen, L.C.; Deelen, J.; Isaacs, A.; Medina-Gomez, C.; Mbarek, H.; Kanterakis, A.; Trompet, S.; Postmus, I.; Verweij, N.; et al. Genome of the Netherlands population-specific imputations identify an ABCA6 variant associated with cholesterol levels. *Nat. Commun.* **2015**, *6*.

89. Kilpeläinen, T.O.; Bentley, A.R.; Noordam, R.; Sung, Y.J.; Schwander, K.; Winkler, T.W.; Jakupović, H.; Chasman, D.I.; Manning, A.; Ntalla, I.; et al. Multi-ancestry study of blood lipid levels identifies four loci interacting with physical activity. *Nat. Commun.* **2019**, *10*.
90. Willer, C.J.; Schmidt, E.M.; Sengupta, S.; Peloso, G.M.; Gustafsson, S.; Kanoni, S.; Ganna, A.; Chen, J.; Buchkovich, M.L.; Mora, S.; et al. Discovery and refinement of loci associated with lipid levels. *Nat. Genet.* **2013**, *45*, 1274–1285.
91. Surakka, I.; Horikoshi, M.; Mägi, R.; Sarin, A.-P.; Mahajan, A.; Lagou, V.; Marullo, L.; Ferreira, T.; Miraglio, B.; Timonen, S.; et al. The impact of low-frequency and rare variants on lipid levels. *Nat. Genet.* **2015**, *47*, 589–597.
92. Forsythe, E.; Beales, P.L. Bardet-Biedl syndrome. *Eur. J. Hum. Genet.* **2013**, *21*, 8–13.
93. Heuckeroth, R.O.; Birkenmeier, E.H.; Levin, M.S.; Gordon, J.I. Analysis of the tissue-specific expression, developmental regulation, and linkage relationships of a rodent gene encoding heart fatty acid binding protein. *J. Biol. Chem.* **1987**, *262*, 9709–9717.
94. Puig-Oliveras, A.; Ramayo-Caldas, Y.; Corominas, J.; Estellé, J.; Pérez-Montarelo, D.; Hudson, N.J.; Casellas, J.; Ballester, J.M.F.M. Differences in muscle transcriptome among pigs phenotypically extreme for fatty acid composition. *PLoS One* **2014**, *9*.
95. Resnyk, C.W.; Carré, W.; Wang, X.; Porter, T.E.; Simon, J.; Le Bihan-Duval, E.; Duclos, M.J.; Aggrey, S.E.; Cogburn, L.A. Transcriptional analysis of abdominal fat in chickens divergently selected on bodyweight at two ages reveals novel mechanisms controlling adiposity: Validating visceral adipose tissue as a dynamic endocrine and metabolic organ. *BMC Genomics* **2017**, *18*, 1–31.
96. Lefterova, M.I.; Zhang, Y.; Steger, D.J.; Schupp, M.; Schug, J.; Cristancho, A.; Feng, D.; Zhuo, D.; Stoeckert, C.J.; Liu, X.S.; et al. PPARγ and C/EBP factors orchestrate adipocyte biology via adjacent binding on a genome-wide scale. *Genes Dev.* **2008**, *22*, 2941–2952.
97. Laplante, M.; Sell, H.; MacNaul, K.L.; Richard, D.; Berger, J.P.; Deshaies, Y. PPAR-gamma activation mediates adipose depot-specific effects on gene expression and lipoprotein lipase activity. *Diabetes* **2003**, *52*, 291–299.
98. Semple, R.K.; Chatterjee, V.K.K.; Rahilly, S.O. PPARγ and human metabolic disease. *J. Clin. Invest.* **2006**, *116*, 581–589.
99. Phua, W.W.T.; Wong, M.X.Y.; Liao, Z.; Tan, N.S. An apparent functional consequence in skeletal muscle physiology via peroxisome proliferator-activated receptors. *Int. J. Mol. Sci.* **2018**, *19*.
100. Wang, Y.X. PPARs: Diverse regulators in energy metabolism and metabolic diseases. *Cell Res.* **2010**, *20*, 124–137.
101. Mitch, W.E.; Medina, R.; Grieber, S.; May, R.C.; England, B.K.; Price, S.R.; Bailey, J.L.; Goldberg, A.L. Metabolic acidosis stimulates muscle protein degradation by activating the adenosine triphosphate-dependent pathway involving ubiquitin and proteasomes. *J. Clin. Invest.* **1994**, *93*, 2127–2133.
102. Medina-Gomez, G.; Gray, S.; Vidal-Puig, A. Adipogenesis and lipotoxicity: Role of peroxisome proliferator-activated receptor γ (PPARγ) and PPARγcoactivator-1 (PGC1). *Public Health Nutr.* **2007**, *10*, 1132–1137.
103. Dammone, G.; Karaz, S.; Lukjanenko, L.; Winkler, C.; Sizzano, F.; Jacot, G.; Migliavacca, E.; Palini, A.; Desvergne, B.; Gilardi, F.; et al. PPARγ Controls Ectopic Adipogenesis and Cross-Talks with Myogenesis During Skeletal Muscle Regeneration. *Int. J. Mol. Sci.* **2018**, *19*, 2044.
104. Wang, Y.H.; Byrne, K.A.; Reverter, A.; Harper, G.S.; Taniguchi, M.; McWilliam, S.M.; Mannen, H.; Oyama, K.; Lehnert, S.A. Transcriptional profiling of skeletal muscle tissue from two breeds of cattle.

Mamm. Genome **2005**, *16*, 201–210.

105. Jeong, J.; Kwon, E.G.; Im, S.K.; Seo, K.S.; Baik, M. Expression of fat deposition and fat removal genes is associated with intramuscular fat content in longissimus dorsi muscle of Korean cattle steers. *J. Anim. Sci.* **2012**, *90*, 2044–2053.
106. Cui, H.; Zheng, M.; Zhao, G.; Liu, R.; Wen, J. Identification of differentially expressed genes and pathways for intramuscular fat metabolism between breast and thigh tissues of chickens. *BMC Genomics* **2018**, *19*, 1–9.
107. Liu, L.; Cui, H.; Fu, R.; Zheng, M.; Liu, R.; Zhao, G.; Wen, J. The regulation of IMF deposition in pectoralis major of fast- and slow- growing chickens at hatching. *J. Anim. Sci. Biotechnol.* **2017**, *8*, 1–8.
108. Kee, H.J.; Kim, J.R.; Nam, K. Il; Hye, Y.P.; Shin, S.; Jeong, C.K.; Shimono, Y.; Takahashi, M.; Myung, H.J.; Kim, N.; et al. Enhancer of polycomb1, a novel homeodomain only protein-binding partner, induces skeletal muscle differentiation. *J. Biol. Chem.* **2007**, *282*, 7700–7709.
109. Shin, C.H.; Liu, Z.P.; Passier, R.; Zhang, C.L.; Wang, D.Z.; Harris, T.M.; Yamagishi, H.; Richardson, J.A.; Childs, G.; Olson, E.N. Modulation of cardiac growth and development by HOP, an unusual homeodomain protein. *Cell* **2002**, *110*, 725–735.
110. Kojic, S.; Nestorovic, A.; Rakicevic, L.; Belgrano, A.; Stankovic, M.; Divac, A.; Faulkner, G. A novel role for cardiac ankyrin repeat protein Ankrd1/CARP as a co-activator of the p53 tumor suppressor protein. *Arch. Biochem. Biophys.* **2010**, *502*, 60–67.
111. Yang, W.; Zhang, Y.; Ma, G.; Zhao, X.; Chen, Y.; Zhu, D. Identification of gene expression modifications in myostatin-stimulated myoblasts. *Biochem. Biophys. Res. Commun.* **2005**, *326*, 660–666.
112. Ma, G.; Wang, H.; Gu, X.; Li, W.; Zhang, X.; Cui, L.; Li, Y.; Zhang, Y.; Zhao, B.; Li, K. CARP, a myostatin-downregulated gene in CFM cells, is a novel essential positive regulator of myogenesis. *Int. J. Biol. Sci.* **2014**, *10*, 309–320.
113. Bagnall, R.D.; Yeates, L.; Semsarian, C. Analysis of the Z-disc genes PDLIM3 and MYPN in Patients with Hypertrophic Cardiomyopathy. *Int. J. Cardiol.* **2010**, *145*, 601–602.
114. Eftestøl, E.; Norman Alver, T.; Gundersen, K.; Bruusgaard, J.C. Overexpression of SMPX in adult skeletal muscle does not change skeletal muscle fiber type or size. *PLoS One* **2014**, *9*.
115. Kostek, M.C.; Chen, Y.-W.; Cuthbertson, D.J.; Shi, R.; Fedele, M.J.; Esser, K.A.; Rennie, M.J. Gene expression responses over 24 h to lengthening and shortening contractions in human muscle: major changes in CSRP3, MUSTN1, SIX1, and FBXO32. *Physiol. Genomics* **2007**, *31*, 42–52.
116. Barash, I.A.; Mathew, L.; Ryan, A.F.; Chen, J.; Lieber, R.L. Rapid muscle-specific gene expression changes after a single bout of eccentric contractions in the mouse. *Am. J. Physiol. Physiol.* **2004**, *286*, C355–C364.
117. Chen, Y.W.; Nader, G.A.; Baar, K.R.; Fedele, M.J.; Hoffman, E.P.; Esser, K.A. Response of rat muscle to acute resistance exercise defined by transcriptional and translational profiling. *J. Physiol.* **2002**, *545*, 27–41.
118. Kemp, T.J.; Sadusky, T.J.; Simon, M.; Brown, R.; Eastwood, M.; Sassoon, D.A.; Coulton, G.R. Identification of a novel stretch-responsive skeletal muscle gene (Smpx). *Genomics* **2001**, *72*, 260–271.
119. MacRae, V.E.; Mahon, M.; Gilpin, S.; Sandercock, D.A.; Mitchell, M.A. Skeletal muscle fibre growth and growth associated myopathy in the domestic chicken (Gallus domesticus). *Br. Poult. Sci.* **2006**, *47*, 264–272.
120. Kuttappan, V.A.; Shivaprasad, H. l.; Shaw, D.P.; Valentine, B.A.; Hargis, B.M.; Clark, F.D.; McKee, S.R.; Owens, C.M. Pathological changes associated with white striping in broiler breast muscles. *Poult. Sci.* **2013**, *92*, 331–338.

121. Lilburn, M.S.; Griffin, J.R.; Wick, M. From muscle to food: oxidative challenges and developmental anomalies in poultry breast muscle. *Poult. Sci.* **2018**.
122. Satriano, J. Kidney growth, hypertrophy and the unifying mechanism of diabetic complications. *Amino Acids* **2007**, *33*, 331–339.
123. Sharma, V.; McNeill, J.H. Diabetic cardiomapathy: Where are we 40 years later? *Can. J. Cardiol.* **2006**, *22*, 305–308.
124. Liang, W.; Menke, A.L.; Driessen, A.; Koek, G.H.; Lindeman, J.H.; Stoop, R.; Havekes, L.M.; Kleemann., R.; Van Den Hoek, A.M. Establishment of a general NAFLD scoring system for rodent models and comparison to human liver pathology. *PLoS One* **2014**, *9*, 1–17.
125. Jingting, S.; Qin, X.; Yanju, S.; Ming, Z.; Yunjie, T.; Gaige, J.; Zhongwei, S.; Jianmin, Z. Oxidative and glycolytic skeletal muscles show marked differences in gene expression profile in Chinese Qingyuan partridge chickens. *PLoS One* **2017**, *12*, 1–17.
126. Palmer, S.; Groves, N.; Schindeler, A.; Yeoh, T.; Biben, C.; Wang, C.-C.; Sparrow, D.B.; Barnett, L.; Jenkins, N.A.; Copeland, N.G.; et al. The Small Muscle-specific Protein Csl Modifies Cell Shape and Promotes Myocyte Fusion in an... *J. Cell Biol.* **2001**, *153*, 985.
127. Tsukada, T.; Pappas, C.T.; Moroz, N.; Antin, P.B.; Kostyukova, A.S.; Gregorio, C.C. Leiomodin-2 is an antagonist of tropomodulin-1 at the pointed end of the thin filaments in cardiac muscle. *J. Cell Sci.* **2010**, *123*, 3136–3145.
128. Pappas, C.T.; Farman, G.P.; Mayfield, R.M.; Konhilas, J.P.; Gregorio, C.C. Cardiac-specific knockout of Lmod2 results in a severe reduction in myofilament force production and rapid cardiac failure. *J. Mol. Cell. Cardiol.* **2018**, *122*, 88–97.
129. Aihara, Y.; Kurabayashi, M.; Saito, Y.; Ohyama, Y.; Tanaka, T.; Takeda, S.; Tomaru, K.; Sekiguchi, K.; Arai, M.; Nakamura, T.; et al. Cardiac ankyrin repeat protein is a novel marker of cardiac hypertrophy: Role of M-CAT element within the promoter. *Hypertension* **2000**, *36*, 48–53.